*Michael Buchwitz (buchwitz@uni-bremen.de)*
*Maximilian Reuter (mreuter@iup.physik.uni-bremen.de)* *Version: 1 (rev 2), 2-June-2016*

# Merged SCIAMACHY/ENVISAT and TANSO-FTS/GOSAT atmospheric column-average dry-air mole fraction of $CO_2$ ($XCO_2$) (XCO2_CRDP3_001)

# Technical Document

## 1. Intent of This Document

This document is intended for users who wish to compare satellite-derived observations with climate model output in the context of the CMIP5/CMIP6//IPCC experiments. It summarizes essential information needed for comparing this dataset to climate model output. References and useful links are provided.

This document describes a satellite-derived atmospheric column-average dry-air mole fraction carbon dioxide ($CO_2$), i.e., $XCO_2$, Level 3 (i.e., gridded) product (in Obs4MIPs format). This product has been obtained from an ensemble of individual Level 2 (i.e., swath) $XCO_2$ products as retrieved from the satellite sensors SCIAMACHY/ENVISAT and TANSO-FTS/GOSAT within the context of the GHG-CCI project (http://www.esa-ghg-cci.org/) of the European Space Agency's (ESA) Climate Change Initiative (CCI). The versions of the Level 2 GHG-CCI data products used as input for this Obs4MIPs product are those of the GHG-CCI "Climate Research Data Package No. 3" (CRDP#3) data set (*Buchwitz et al., 2016b*; data available from http://www.esa-ghg-cci.org/).

The Level 3 Obs4MIPs $XCO_2$ product described in this document has been specifically generated for comparisons with climate model output.

*Dataset Filename:*
*xco2_ghgcci_l3_v100_200301_201412.nc*
*Link (preliminary):*
*http://www.iup.uni-bremen.de/~mreuter/xco2_ghgcci_l3_v100_200301_201412.nc*
*Ancillary Files:*
*None*
*Technical Point of Contact:*
*Maximilian Reuter, Inst. of Environmental Physics (IUP), Univ. Bremen, Germany,*
*mreuter@iup.physik.uni-bremen.de*
*Michael Buchwitz, Inst. of Environmental Physics (IUP), Univ. Bremen, Germany,*
*buchwitz@uni-bremen.de*

## 2. Data Origin and Field Description

The main quantity / data field is the column-average dry-air mole fraction of atmospheric carbon dioxide ($CO_2$), denoted $XCO_2$, as retrieved from the two satellite instruments SCIAMACHY/ENVISAT (*Burrows et al., 1995; Bovensmann et al., 1999*) and TANSO-FTS/GOSAT (*Kuze et al., 2009*). $XCO_2$ is a dimensionless quantity (unit: mol/mol) defined as the vertical column of $CO_2$ divided by the vertical column of dry air (= all air molecules except water vapor) (see, e.g., *Buchwitz et al., 2005*, for details). For example, if $XCO_2$ is 0.0004 (i.e., 400 ppm, parts per million) at a given location this means that there are 400 $CO_2$ molecules above that location per 1 million air molecules (excluding water vapor molecules).

$XCO_2$ is retrieved from radiance spectra located in the near-infrared/short-wave infrared (NIR/SWIR) spectral region of the electro-magnetic spectrum using (mostly) Optimal Estimation (*Rodgers, 2000*) retrieval algorithms (see Tab. 2). Each algorithm has an underlying radiative transfer model and a number of fit parameters (the co-called state vector elements), which are iteratively adjusted until the simulated radiance spectrum gives an optimal fit to the observed radiance spectrum (considering, e.g., instrument noise and *a priori* knowledge on atmospheric parameters). For details please see the

Algorithm Theoretical Baseline Documents (ATBDs) as given on the GHG-CCI website for each individual Level 2 data product (see links to ATBDs in product tables on GHG-CCI main data products website: http://www.esa-ghg-cci.org/sites/default/files/documents/public/documents/GHG-CCI_DATA.html).

The key characteristics of this Obs4MIPs $XCO_2$ data product are shown in Tab. 1:

| | |
|---|---|
| **CF variable name, units** | Long name: column-average dry-air mole fraction of atmospheric carbon dioxide<br>Standard name: dry_atmosphere_mole_fraction_of_carbon_dioxide<br>Units: dimensionless (mol/mol)<br><br>See also: CF Standard Name Table, Version 31, 08 March 2016 (http://cfconventions.org/Data/cf-standard-names/31/build/cf-standard-name-table.html) |
| **Spatial resolution** | 5° equal angle |
| **Temporal resolution** | Monthly average, from January 2003–December 2014 |
| **Coverage** | Global (2003 – mid 2009: land only) |

**Tab. 1:** Main characteristics of the $XCO_2$ Obs4MIPs product.

Note that a resolution of $5^o$x$5^o$ has been selected (instead of, e.g., $1^o$x$1^o$) to ensure better noise suppression (note that the underlying individual satellite retrievals are noisy and sparse due to very strict quality filtering).

The main variables as contained in the $XCO_2$ Obs4MIPs product file are:

*xco2:*
Satellite retrieved column-average dry-air mole fraction of atmospheric carbon dioxide (Note: typical values are << 1.0 (typically close to 0.0004) and 1.0E20 = no data)

*xco2_nobs:*
Number of individual $XCO_2$ Level 2 observation (per $5^o$x$5^o$ grid cell) used to compute the reported Level 3 $XCO_2$ monthly average value (0 = no data)

*xco2_stderr:*
Reported uncertainty defined as standard error of the average including single sounding noise and potential seasonal and regional biases

*xco2_stddev:*
Average standard deviation of the underlying $XCO_2$ Level 2 observations

*time:*
Time in days since 1-Jan-1990

*lat:*
Center latitude in degrees north (-90.0 to +90.0)

*lon:*
Center longitude in degrees east (-180.0 to +180.0)

## 3. Data Product Algorithm Overview

As already mentioned, the Obs4MIPs product has been generated using individual satellite sensor Level 2 $XCO_2$ products as input. These input data, which are all part of the GHG-CCI CRDP3 data set (*Buchwitz et al., 2016b*), are the following $XCO_2$ Level 2 data products:

| **GHG-CCI Level 2 $XCO_2$ algorithms / products used as input data for the generation of the Obs4MIPs product** | | | |
|---|---|---|---|
| **Algorithm ID (Version)** | **Sensor** | **Algorithm Institute** | **Comment (Reference)** |
| CO2_SCI_BESD (v02.01.01) | SCIAMACHY/ ENVISAT | BESD IUP, Univ. Bremen | Coverage: global (land), 1.2003-3.2012 (*Reuter et al., 2011*) |
| CO2_SCI_WFMD (v3.9) | SCIAMACHY/ ENVISAT | WFM-DOAS IUP, Univ. Bremen | Coverage: global (land), 1.2003-4.2012 (*Schneising et al., 2011*) |
| CO2_GOS_OCFP (v6.0) | TANSO/GOSAT | UoL-FP Univ. Leicester | Coverage: global, 4.2009-12.2014 (Cogan et al., 2012) |
| CO2_GOS_SRFP (v2.3.7) | TANSO/GOSAT | RemoTeC SRON/KIT | Coverage: global, 6.2009-12.2014 (*Butz et al., 2011*) |

**Tab. 2:** Overview of the Level 2 $XCO_2$ products used as input for the generation of the Level 3 Obs4MIPs $XCO_2$ product.

From the individual sensor/algorithm Level 2 (L2) $XCO_2$ input data the Level 3 (L3) Obs4MIPs product has been generated as follows: To correct for the use of different $CO_2$ *a priori* assumptions in the independently retrieved products, all products have been brought to a common *a priori* using the Simple Empirical $CO_2$ Model (SECM) described in *Reuter et al., 2012*. After this a gridded L3 product is generated for each L2 product by averaging all soundings falling into $5^o x 5^o$ monthly grid cells. Only those grid cells are further considered having a standard error of the mean of smaller than 2 ppm. The grid cell uncertainty is computed from the reported L2 uncertainties and a term accounting for potential regional / temporal biases (see *Buchwitz et al., 2016a*). To avoid potential "jumps" in the Obs4MIPs product, each L3 product has been offset corrected in the overlap period using the mean of the products as reference (conserving the mean value). The observed offsets are small and always between -0.4 ppm and +0.6 ppm.

The Obs4MIPs $XCO_2$ value in a given grid cell is computed as the mean of the individual L3 values and the corresponding reported uncertainty is the root-mean-square of the individual L3 uncertainties. Finally a filtering procedure has been applied to remove "unreliable" grid cells considering the overall noise error (1.6 ppm) and total uncertainty (1.8 ppm) of each cell.

## 4. Validation and Uncertainty Estimates

As described in the Sect. 2, an $XCO_2$ uncertainty value (*xco2_stderr*) is contained in the Obs4MIPs file for each grid cell with valid data (*xco2* $< 1.0E20$ and/or *xco2_nobs* $> 0$, see above). How this uncertainty has been estimated is described in Sect. 3.

In order to validate this product it has been compared with Total Carbon Column Observation Network (TCCON, *Wunch et al., 2011*) ground-based $XCO_2$ retrievals using version GGG2014 (*Wunch et al., 2015*) at six TCCON sites (2 in the USA (Park Falls and Lamont), 2 in Europe (Bremen and Bialystok) and 2 in Australia (Darwin and Wollongong)).

Fig. 1 shows a summary of the results. As can be seen, the agreement with the reference data is 0.29 +/- 1.2 ppm (1-sigma). As can also be seen, the distribution of the errors is close to a normal distribution with mean value 0.29 ppm and standard deviation 1.2 ppm.

The mean value of the reported uncertainty (“Mean Serr”) is 0.67 ppm. Note that the standard deviation of the difference to TCCON is larger (1.2 ppm) than this value, e.g., due to the uncertainty of the TCCON reference data (0.4 ppm) but also for other reasons, e.g., non-perfect spatio-temporal colocation of the satellite and the TCCON data, representativity error (see Sect. 5) and for other reasons.

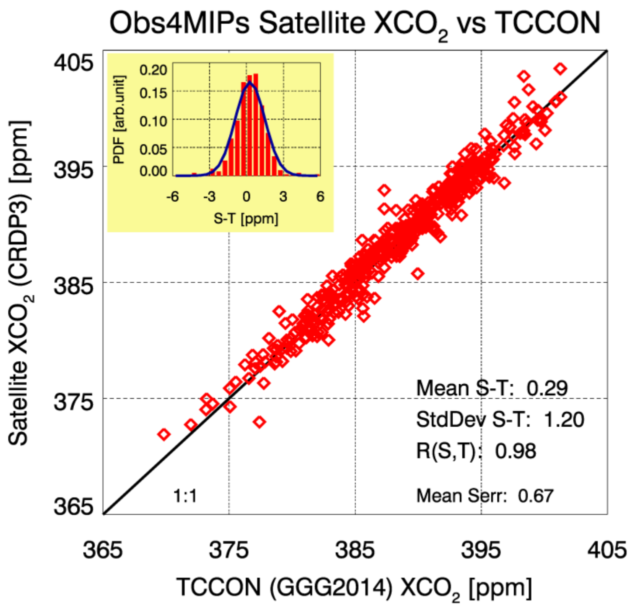


**Fig. 1:** Summary of the validation of the Obs4MIPs product using TCCON ground-based $XCO_2$ retrievals. As can be seen, the mean value of the difference (satellite-TCCON) is 0.29 ppm and the standard deviation of the difference is 1.2 ppm. The mean value of the reported uncertainty (“Mean Serr”) is 0.67 ppm and the correlation coefficient, R, is 0.98. The inserted figure top-left shows the distribution of the satellite-TCCON differences (red bars) compared to a normal distribution with mean 0.29 ppm and standard deviation 1.2 ppm.

## 5. Considerations for Model-Observation Comparisons

Satellite $XCO_2$ products are typically used in combination with $CO_2$ surface flux inverse modelling approaches to obtain information on $CO_2$ surface fluxes by using a (global or regional) transport model with free fit parameters (primarily regional surface fluxes) (e.g., *Basu et al., 2013; Chevallier et al., 2014; Reuter et al., 2014; Houweling et al., 2015*). The satellite data can also be used to constrain process parameters of a terrestrial biosphere model, e.g., as part of a Carbon Cycle Data Assimilation System (CCDAS, e.g., *Kaminski et al., 2013*)) or for direct comparisons with global climate models.

Strictly speaking, this requires taking the exact time and location of the satellite observations into account as well as the altitude sensitivity. Note for example, that the satellite retrievals are limited to clear sky observations around local noon and that this needs to be considered for satellite – model comparisons.

The altitude sensitivity can be considered by applying the satellite $XCO_2$ averaging kernels to the model $CO_2$ vertical profiles (see, e.g., *Buchwitz et al., 2014*, for details). User who would like to consider all this should use the available Level 2, i.e., individual observation, data products. Level 2 $XCO_2$ products from SCIAMACHY and GOSAT are available via the GHG-CCI website (http://www.esa-ghg-cci.org/), GOSAT $XCO_2$ is available from NIES (http://www.gosat.nies.go.jp/en/) and from NASA/ACOS (http://disc.sci.gsfc.nasa.gov/acdisc/documentation/ACOS.html ). $XCO_2$ from NASA’s OCO-2 mission is available from http://oco.jpl.nasa.gov/science/OCO2DataCenter/. Note that the $XCO_2$ Level 2 products used for the described Obs4MIPs product are the ones from GHG-CCI and that the other products (from NIES and NASA) have been generated using different algorithms.

Due to the gridding / averaging process needed to generate Obs4MIPs products detailed time/location information is not available in the Obs4MIPs data product. Also averaging kernels are not (yet) part of these products (it requires research to find out how to generate appropriate averaging kernels for Obs4MIPs products and related information, which is also needed in order to properly use averaging kernels). Note that the Obs4MIPs satellite – model comparison philosophy is based on generating satellite and model parameters (such as $XCO_2$) which can be compared directly. This approach has pros and cons – it is convenient but has limitations, depending on application.

Fortunately, the satellite $XCO_2$ averaging kernels are close to unity (especially in the lower troposphere, where the $CO_2$ variability is typically largest). Therefore applying the averaging kernels typically changes the $XCO_2$ values by much less than 1 ppm (see, e.g, *Dils et al., 2014*). However, how large this "correction" is depends (also) on the difference between the *a priori* $CO_2$ profile used for satellite retrieval and the model $CO_2$ profile. The larger this difference, the large the averaging kernel correction. If the model profiles are "reasonable" other error sources are likely more relevant for using the Obs4MIPs product such as the representativity error. A representativity error originates from the fact that the "true" $XCO_2$ field is variable within a given month in a given grid cell but the Obs4MIPs values are derived from averaging sparse satellite observations, i.e., are not representative for the "true" monthly mean value of a given grid cell. Note that the validation results reported in the previous section (agreement with ground-based observations within 0.29 +/- 1.2 ppm (1-sigma)) have also been obtained without considering the averaging kernels and the established difference includes (at least to some extent) the representativity error as well as other error sources (e.g., the uncertainty of the TCCON reference observations, which is 0.4 ppm (1-sigma)). It still needs to be investigated in detail how large exactly these error sources are for a typical application of this Obs4MIPs product but for now it is recommended to use the reported overall uncertainty range of 0.29 +/- 1.2 ppm (1-sigma) (see Sect. 4) and/or the reported uncertainties for each grid cell as given in the Obs4MIPs product file.

Overall it can therefore be expected that model minus satellite differences larger than approximately 2-3 ppm point to significant issues with the model $XCO_2$ values (differences are significant at the 5% significance level if outside of the 2-sigma (95%) uncertainty range of [-2.1 ppm, 2.7 ppm]).

Note however that the $XCO_2$ Obs4MIPs product is new and that not all possible assessments have been carried out yet. The product has been generated by merging an ensemble of underlying Level 2 products (see Tab. 2 and consult the relevant publications referred to in Tab. 2 and additional technical information available on http://www.esa-ghg-cci.org/ for details on each algorithm / product). No obvious issues have been identified (see, e.g., figures in this document) but it cannot be excluded that there are potential issues (depending on data usage / application) due to merging different data sets (see, e.g., following section with Fig. 5, bottom, showing the drop of the number of observations beginning 2012 due to the loss of data from SCIAMACHY/ENVISAT).

How to compute $XCO_2$ from model data depends on the model but here a general procedure how to compute model $XCO_2$ for comparison with the satellite-based Obs4MIPs product:

$$XCO_2 = \frac{\sum n_d \cdot c_{CO_2}}{\sum n_d}$$

Here, $c_{CO_2}$ represents the modeled $CO_2$ dry air mole fraction on model layers (i.e., layer centers or full levels) and $n_d$ the number of dry air particles (air molecules excluding water vapor) within these layers. The summations are performed over all model layers. The number of dry air particles can be computed as follows:

$$n_d = \frac{N_a \cdot \Delta p \cdot (1 - q)}{m_d \cdot g}$$

$N_a$ is the Avogadro constant ($6.022140857 \cdot 10^{23}\ mol^{-1}$) and $m_d$ the molar mass of dry air ($28.9644 \cdot 10^{-3}\ kg\ mol^{-1}$). $\Delta p$ is the pressure difference (in hPa) computed from the model's pressure levels (i.e., layer boundaries or half levels) surrounding the model layers, $q$ is the modeled specific humidity (in $kg/kg$), and $g$ the gravitational accelaration approximated by:

$$g = g_0^2 + 2 \cdot f \cdot \phi$$

This includes the model's geopotential $\phi$ (in $m^2 s^{-2}$) on layers, the free air correction constant $f = 3.0825958 \cdot 10^{-6}\ s^{-2}$, and the gravitational acceleration $g_0$ on the geoid approximated by the international gravity formula depending only on the latitude $\varphi$:

$$g_0 = 9.780327 \cdot [1 + 0.0053024 \cdot \sin^2(\varphi) - 0.0000058 \cdot \sin^2(2\varphi)]$$

### 5.1 Monthly $XCO_2$ Distribution and Time Series Examples

Figure 2 shows as an example the $XCO_2$ distribution, the number of observations, the reported $XCO_2$ uncertainty and the $XCO_2$ standard deviation for August 2010. As can be seen, $XCO_2$ is typically lower over mid and high latitudes of the northern hemisphere (compared to the southern hemisphere) as during northern hemisphere summer large amounts of atmospheric $CO_2$ are taken up by the growing terrestrial vegetation especially at mid and high latitudes. As can also be seen, the number of observations depends significantly on location with largest values over locations with low cloud cover, high surface reflectivity and (at least) moderate to high sun elevation. Over ocean coverage is sparse as ocean retrievals are only included from GOSAT sun-glint mode observations (outside of glint conditions the reflectivity of water is very low in the NIR/SWIR spectral region). The reported uncertainty also depends on location with best values (lowest numbers) for locations with highest surface reflectivity (e.g., deserts).

Figures 3 and 4 show the corresponding maps for August 2008 (Fig. 3) and August 2012 (Fig. 4), where $XCO_2$ is on average about 4 ppm lower (2008) or higher (2012) due to the approximately 2 ppm/year increase resulting from anthropogenic $CO_2$ emissions (and an approximately 50% uptake by land and ocean sinks). Note that prior to mid 2009 the Obs4MIPs product is limited to observations over land due to the availability of SCIAMACHY data only (GOSAT ocean sun-glint mode observations are only available after mid 2009).

Figure 5 shows $XCO_2$ time series for three latitude bands, the corresponding mean value of the reported uncertainty, the standard deviation and the number of observations.

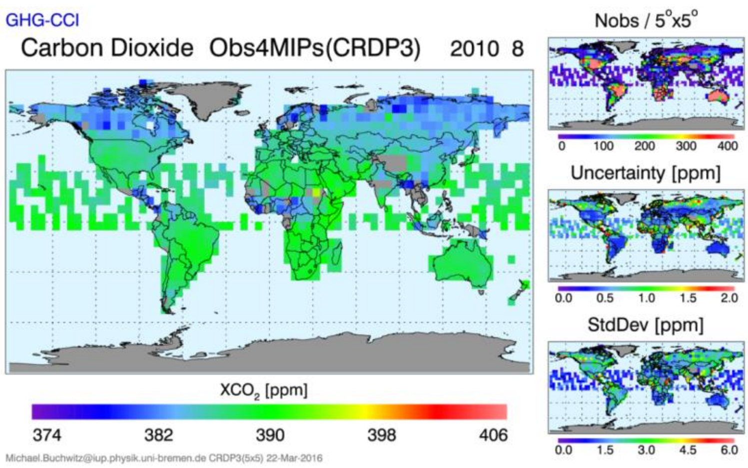


**Fig. 2:** Left: Obs4MIPs $XCO_2$ for August 2010. Right: Top: Number of observations per $5^o$x$5^o$ grid cell. Middle: Reported $XCO_2$ uncertainty. Bottom: $XCO_2$ standard deviation.

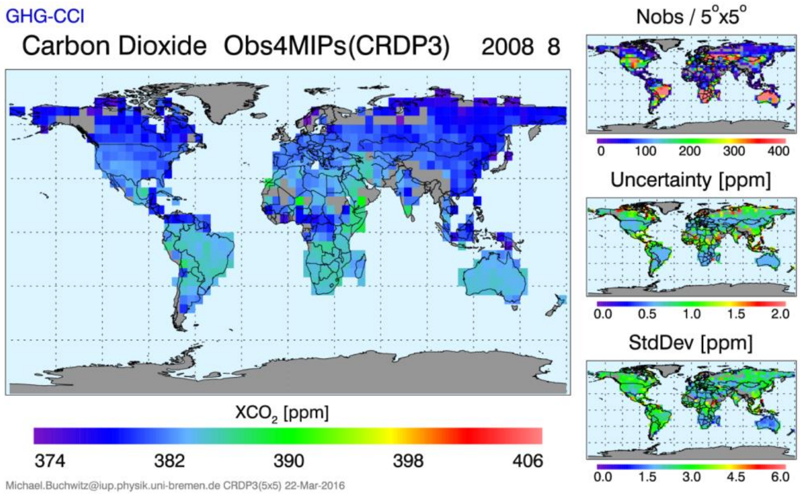


**Fig. 3:** As Fig.2 but for August 2008.

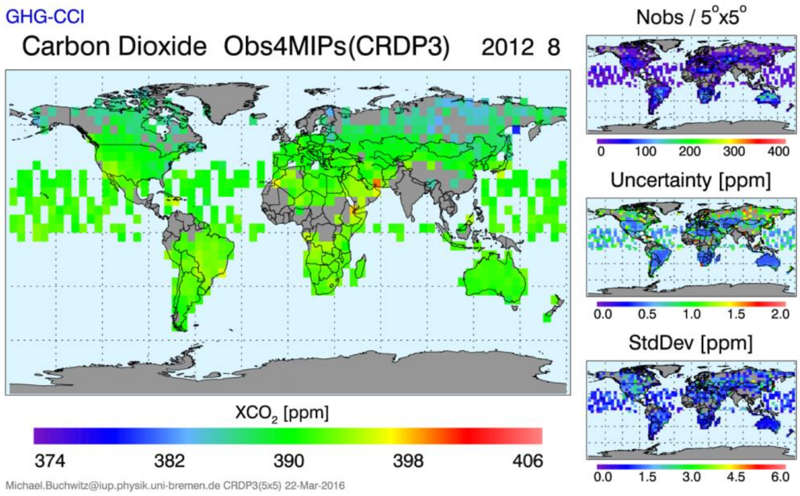


**Fig. 4:** As Fig.2 but for August 2012.

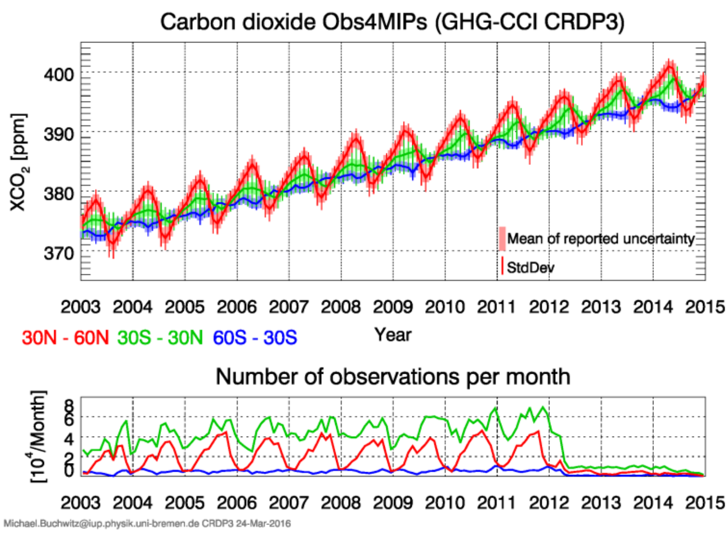


**Fig. 5:** Timeseries of monthly $XCO_2$ for three latitude bands (top) and corresponding number of observations (bottom). The drop of the number of observations in 2012 is because of the end of the SCIAMACHY/ENVISAT time series.

### 5.2 Spatio-temporal Sampling

The spatio-temporal sampling of the satellite data is typically sparse (see Figs. 2-4) as the satellite retrievals are strictly quality-filtered to avoid (even very small) cloud (and aerosol) contamination. Furthermore, water and snow/ice are poor reflectors in the NIR/SWIR spectral region and, therefore, the retrievals are (typically) limited to water and snow and ice free land surfaces (exception: sun-glint conditions as explained above). In addition other requirements are also important, in particular the solar zenith angle (SZA) needs to be "small enough" (e.g., below $70^o$, i.e., the sun needs to be high enough above the horizon to have appropriate illumination conditions).

Note also that the satellite observations are obtained around local noon (around 10:00 a.m. local time for SCIAMACHY/ENVISAT and around 1:00 p.m. local time for TANSO-FTS/GOSAT). More details on the satellite instruments is provided in the following section.

## 6. Instruments Overview

In the following two sub-sections a short overview about the SCIAMACHY/ENVISAT and TANSO-FTS/GOSAT satellite instruments is given.

### 6.1 SCIAMACHY/ENVISAT

The SCIAMACHY instrument (*Burrows et al., 1995; Bovensmann et al., 1999*) was a German, Dutch and Belgian instrument contribution to ESA's ENVISAT, which flew in a sun-synchronous orbit in descending node, crossing the equator at 10:00 a.m. local time during the time period 2002 to April 2012. SCIAMACHY was a grating spectrometer, which measured solar radiation, reflected at the Earth's surface, backscattered from the atmosphere, transmitted through the atmosphere, or emitted from the atmosphere in the ultraviolet, visible, and NIR/SWIR spectral regions (240–1750 nm, 1940–2040 nm, 2265–2380 nm) at moderate spectral resolution (0.2–1.4 nm). SCIAMACHY observed the Earth's atmosphere in various viewing geometries. Of relevance for this technote is the nadir viewing mode (down-looking) and the 1558–1594 nm and 755–775 nm spectral regions containing molecular $CO_2$ and oxygen ($O_2$) absorption lines. The column-averaged dry air mole fraction of $CO_2$, $XCO_2$, is calculated from the retrieved columns of $CO_2$ and $O_2$ (e.g., *Reuter et al., 2010*). The horizontal resolution, i.e., the size of a single ground pixel, is typically 30 km along track (approximately north-south) times 60 km across track (approximately east-west). On the Earth's day side an alternating sequence of nadir and limb measurements had been performed. Full longitudinal (global) coverage in nadir was achieved at the equator in six days and more rapidly at higher latitudes. As shown in, e.g., *Buchwitz et al., 2005*, the sensitivity of the SCIAMACHY $CO_2$ measurements is only weakly dependent on altitude throughout the troposphere and down to the Earth's surface. The latter is a pre-requisite to obtain regional $CO_2$ source/sink information, which is the main scientific goal of the SCIAMACHY $CO_2$ measurements (e.g., *Reuter et al., 2014*).

### 6.2 TANSO-FTS/GOSAT

GOSAT (*Kuze et al., 2009*), also called "Ibuki", is the first satellite in orbit specifically designed to deliver high-quality column-averaged dry air mole fractions of $CO_2$ and $CH_4$, i.e., $XCO_2$ and $XCH_4$. GOSAT flies at an altitude of approximately 666 km and completes one revolution in about 100 minutes. The local sun time at equator crossing is around 12:45 – 13:15 PM. The satellite returns to the same point in space in three days. The observation instrument onboard the satellite is the Thermal And Near-infrared Sensor for carbon Observation (TANSO). TANSO is composed of two subunits: the Fourier Transform Spectrometer (FTS) and the Cloud and Aerosol Imager (CAI). The main instrument as used for the purpose of this technote is TANSO-FTS. Similar as SCIAMACHY, TANSO-FTS observes infrared light reflected and emitted from the earth's surface and the atmosphere. However, the radiance spectra as measured by TANSO-FTS are obtained at a much higher spectral resolution compared to SCIAMACHY and the ground pixel size is smaller (10 km compared to 60 km for SCIAMACHY). The number of observations is however much lower compared to SCIAMACHY as one observation typically requires 4s whereas SCIAMACHY obtained several spectra during this time period. Also the scan pattern differs from SCIAMACHY (GOSAT: typically 5 or 3 non-consecutive ground pixels along the swath whereas SCIAMACHY has a gap-free scan pattern across a wider swath). For details we refer to *Kuze et al., 2009*, and to JAXA (http://global.jaxa.jp/projects/sat/gosat/) and NIES (http://www.gosat.nies.go.jp/eng/gosat/page5.htm) GOSAT websites for latest information.

## 7. References


Basu, S., S. Guerlet, A. Butz, et al., 2013, Global $CO_2$ fluxes estimated from GOSAT retrievals of total column $CO_2$, Atmos. Chem. Phys., 13, 8695-8717.

Bovensmann, H., J. P. Burrows, M. Buchwitz, et al., 1999, SCIAMACHY - Mission objectives and measurement modes, J. Atmos. Sci., 56, (2), 127-150.

Buchwitz, M., R. de Beek, J. P. Burrows, et al. (2005), Atmospheric methane and carbon dioxide from SCIAMACHY satellite data: Initial comparison with chemistry and transport models, Atmos. Chem. Phys., 5, 941-962. Link: http://www.atmos-chem-phys.org/5/941/2005/acp-5-941-2005.pdf

Buchwitz, M., Detmers, R., Boesch, H., et al. (2014), Product Specification Document for the GHG-CCI project of ESA's Climate Change Initiative, version 3 (PSDv3), 6. June 2014. Link: http://www.esa-ghg-cci.org/index.php?q=webfm_send/160

Buchwitz, M., M. Reuter, O. Schneising, et al. (2015a), The Greenhouse Gas Climate Change Initiative (GHG-CCI): comparison and quality assessment of near-surface-sensitive satellite-derived $CO_2$ and $CH_4$ global data sets, *Remote Sensing of Environment*, 162, 344-362, doi:10.1016/j.rse.2013.04.024. Link: http://www.sciencedirect.com/science/article/pii/S0034425713003520

Buchwitz, M., et al. (2016a), ESA Climate Change Initiative (CCI) Product Validation and Intercomparison Report (PVIR) for the Essential Climate Variable (ECV) Greenhouse Gases (GHG) for data set Climate Research Data Package No. 3 (CRDP#3), *technical report*, Version 4.0, 24 Feb 2016, link: http://www.esa-ghg-cci.org/?q=webfm_send/300

Buchwitz, M., et al. (2016b), Global satellite observations of column-averaged carbon dioxide and methane: The GHG-CCI XCO2 and XCH4 CRDP3 data set, manuscript in preparation for *Remote Sensing of Environment* Special Issue on "Earth Observation of Essential Climate Variables"

Burrows, J. P., Hölzle, E., Goede, A. P. H., Visser, H., and Fricke, W. (1995), SCIAMACHY – Scanning Imaging Absorption Spectrometer for Atmospheric Chartography, *Acta Astronautica*, 35(7), 445–451.

Butz, A., Guerlet, S., Hasekamp, O., Schepers, D., et al. (2011), Towards accurate CO2 and CH4 observations from GOSAT, Geophys. Res. Lett., doi:10.1029/2011GL047888. Link: http://onlinelibrary.wiley.com/doi/10.1029/2011GL047888/abstract

Chevallier, F., Palmer, P.I., Feng, L., Boesch, H., O'Dell, C.W., Bousquet, P., et al. (2014), Towards robust and consistent regional $CO_2$ flux estimates from in situ and space-borne measurements of atmospheric $CO_2$, Geophys. Res. Lett., 41, 1065-1070, DOI: 10.1002/2013GL058772.

Cogan, A. J., Boesch, H., Parker, R. J., et al. (2012), Atmospheric carbon dioxide retrieved from the Greenhouse gases Observing SATellite (GOSAT): Comparison with ground-based TCCON observations and GEOS-Chem model calculations, J. Geophys. Res., 117, D21301, doi:10.1029/2012JD018087. Link: http://onlinelibrary.wiley.com/doi/10.1029/2012JD018087/abstract

Dils, B., M. Buchwitz, M. Reuter, et al. (2014), The Greenhouse Gas Climate Change Initiative (GHG-CCI): comparative validation of GHG-CCI SCIAMACHY/ENVISAT and TANSO-FTS/GOSAT $CO_2$ and $CH_4$ retrieval algorithm products with measurements from the TCCON, *Atmos. Meas. Tech.*, 7, 1723-1744. Link: http://www.atmos-meas-tech.net/7/1723/2014/amt-7-1723-2014.html

Houweling, S., D. Baker, S. Basu, et al. ( 2015), An intercomparison of inverse models for estimating sources and sinks of $CO_2$ using GOSAT measurements, J. Geophys. Res. Atmos., 120, 5253–5266, doi:10.1002/2014JD022962.

Kaminski, T., W. Knorr, G. Schürmann, M. Scholze, P. J. Rayner, S. Zaehle, S. Blessing, W. Dorigo, V. Gayler, R. Giering, N. Gobron, J. P. Grant, M. Heimann, A. Hooker-Strout, S. Houweling, T. Kato, J. Kattge, D. Kelley, S. Kemp, E. N. Koffi, C. Köstler, P.P. Mathieu, B. Pinty, C. H. Reick, C. Rödenbeck, R. Schnur, K. Scipal, C. Sebald, T. Stacke, A. Terwisscha van Scheltinga, M. Vossbeck, H. Widmann, and T. Ziehn (2013), The BETHY/JSBACH Carbon Cycle Data Assimilation System: experiences and challenges. J. Geophys. Res., 118:doi:10.1002/jgrg.20118.

Kulawik, S. S., D. Wunch, C. O'Dell, et al. (2016), Consistent evaluation of GOSAT, SCIAMACHY, CarbonTracker, and MACC through comparisons to TCCON, *Atmos. Meas. Tech.*, 9, 683-709, doi:10.5194/amt-9-683-2016.

Kuze, A., Suto, H., Nakajima, M., and Hamazaki, T. (2009), Thermal and near infrared sensor for carbon observation Fourier-transform spectrometer on the Greenhouse Gases Observing Satellite for greenhouse gases monitoring, *Appl. Opt.*, 48, 6716–6733.

Reuter, M., Buchwitz, M., Schneising, O., Heymann, J., Bovensmann, H., Burrows, J. P. (2010), A method for improved SCIAMACHY $CO_2$ retrieval in the presence of optically thin clouds, *Atmos. Meas. Tech.*, 3, 209-232. Link: http://onlinelibrary.wiley.com/doi/10.1029/2010JD015047/abstract

Reuter, M., Bovensmann, H., Buchwitz, M., Burrows, J. P. (2011), Retrieval of atmospheric $CO_2$ with enhanced accuracy and precision from SCIAMACHY: Validation with FTS measurements and comparison with model results, *J. Geophys. Res.*, 116, D04301, doi:10.1029/2010JD015047. Link: http://www.atmos-meas-tech.net/3/209/2010/amt-3-209-2010.pdf

Reuter, M., M. Buchwitz, O. Schneising, F. Hase, J. Heymann, S. Guerlet, A. J. Cogan, H. Bovensmann, and J. P. Burrows (2012), A simple empirical model estimating atmospheric $CO_2$ background concentrations, Atmos. Meas. Tech., 5, 1349-1357, 2012.

Reuter, M., H. Boesch, H. Bovensmann, A. Bril, M. Buchwitz, et al. (2013), A joint effort to deliver satellite retrieved atmospheric $CO_2$ concentrations for surface flux inversions: the ensemble median algorithm EMMA, Atmos. Chem. Phys., 13, 1771-1780. Link: http://www.atmos-chem-phys.net/13/1771/2013/acp-13-1771-2013.pdf

Reuter, M., Buchwitz, M., Hilker, M., et al. (2014), Satellite-inferred European carbon sink larger than expected, Atmos. Chem. Phys., 14, 13739-13753, www.atmos-chem-phys.net/14/13739/2014/, doi:10.5194/acp-14-13739-2014. Link: http://www.atmos-chem-phys.net/14/13739/2014/acp-14-13739-2014.html

Rodgers, C. D. (2000), Inverse Methods for Atmospheric Sounding: Theory and Practice, World Scientific Publishing.

Schneising, O., Buchwitz, M., Reuter, M., Heymann, J., Bovensmann, H., and Burrows, J. P. (2011), Long-term analysis of carbon dioxide and methane column-averaged mole fractions retrieved from SCIAMACHY, Atmos. Chem. Phys., 11, 2881-2892.

Schneising, O., Bergamaschi, P., Bovensmann, H., Buchwitz, M., et al. (2012), Atmospheric greenhouse gases retrieved from SCIAMACHY: comparison to ground-based FTS measurements and model results, Atmos. Chem. Phys., 12, 1527-1540. Link: http://www.atmos-chem-phys.net/12/1527/2012/acp-12-1527-2012.pdf

Schneising, O., Reuter, M., Buchwitz, M., Heymann, J., Bovensmann, H., and Burrows, J. P. (2014), Terrestrial carbon sink observed from space: variation of growth rates and seasonal cycle amplitudes in response to interannual surface temperature variability, Atmos. Chem. Phys., 14, 133-141. Link: http://www.atmos-chem-phys.net/14/133/2014/

Wunch, D., Toon, G. C., Blavier, J.-F. L., Washenfelder, R. A., Notholt, J., Connor, B. J., Griffith, D. W. T., Sherlock, V., Wennberg, P. O. (2011), The Total Carbon Column Observing Network, Phil. Trans. R. Soc. A, 369, 2087–2112, doi:10.1098/rsta.2010.0240.

Wunch, D., Toon, G. C., Sherlock, V., Deutscher, N. M, Liu, X., Feist, D. G., and Wennberg, P. O. (2015), The Total Carbon Column Observing Network's GGG2014 Data Version. Carbon Dioxide Information Analysis Center, Oak Ridge National Laboratory, Oak Ridge, Tennessee, USA, available at: doi:10.14291/tccon.ggg2014.documentation.R0/1221662.

## 8. Useful Links

SCIAMACHY website: http://www.iup.uni-bremen.de/sciamachy/
GOSAT website: http://global.jaxa.jp/projects/sat/gosat/
ESA GHG-CCI project website: http://www.esa-ghg-cci.org/
IUP-UB CarbonGroup: http://www.iup.uni-bremen.de/sciamachy/NIR_NADIR_WFM_DOAS/

## 9. Revision History

Version 1, Revision 2 – 06/02/2016 – Initial release (reviewed).

***** end of document**